

# SDSS-IV MaNGA: The Different Quenching Histories of Fast and Slow Rotators

R. J. Smethurst,<sup>1</sup> K. L. Masters,<sup>2</sup> C. J. Lintott,<sup>3</sup> A. Weijmans,<sup>4</sup> M. Merrifield,<sup>1</sup>  
 S. J. Penny,<sup>2</sup> A. Aragón-Salamanca,<sup>1</sup> J. Brownstein,<sup>5</sup> K. Bundy,<sup>6</sup> N. Drory,<sup>7</sup>  
 D. R. Law,<sup>8</sup> R. C. Nichol<sup>2</sup>

<sup>1</sup> *School of Physics and Astronomy, The University of Nottingham, University Park, Nottingham, NG7 2RD, UK*

<sup>2</sup> *Institute of Cosmology and Gravitation, University of Portsmouth, Dennis Sciama Building, Barnaby Road, Portsmouth, PO13FX, UK*

<sup>3</sup> *Oxford Astrophysics, Department of Physics, University of Oxford, Denys Wilkinson Building, Keble Road, Oxford, OX13RH, UK*

<sup>4</sup> *School of Physics and Astronomy, University of St Andrews, North Haugh, St Andrews, Fife, KY169RJ, UK*

<sup>5</sup> *Department of Physics and Astronomy, University of Utah, 115 S. 1400 E., Salt Lake City, UT 84112, USA*

<sup>6</sup> *University of California, Santa Cruz, 1156 High St. Santa Cruz, CA 95064, USA*

<sup>7</sup> *McDonald Observatory, The University of Texas at Austin, 1 University Station, Austin, TX 78712, USA*

<sup>8</sup> *Space Telescope Science Institute, 3700 San Martin Drive, Baltimore, MD 21218, USA*

*Accepted 2017 September 25. Received 2017 September 25; in original form 2017 August 25.*

28 September 2017

	Internal Processes ('Nature')	External Processes ('Nurture')
Fast quenching	AGN feedback	Mergers
Intermediate quenching	Mass quenching	Environmental quenching
Slow quenching	Morphological quenching	Gas accretion

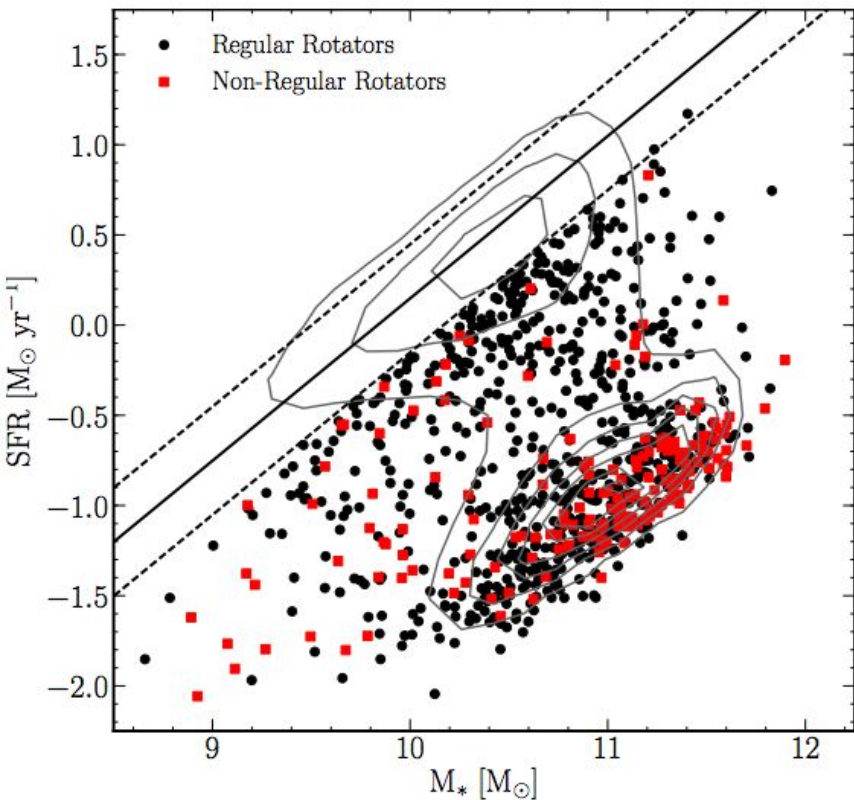
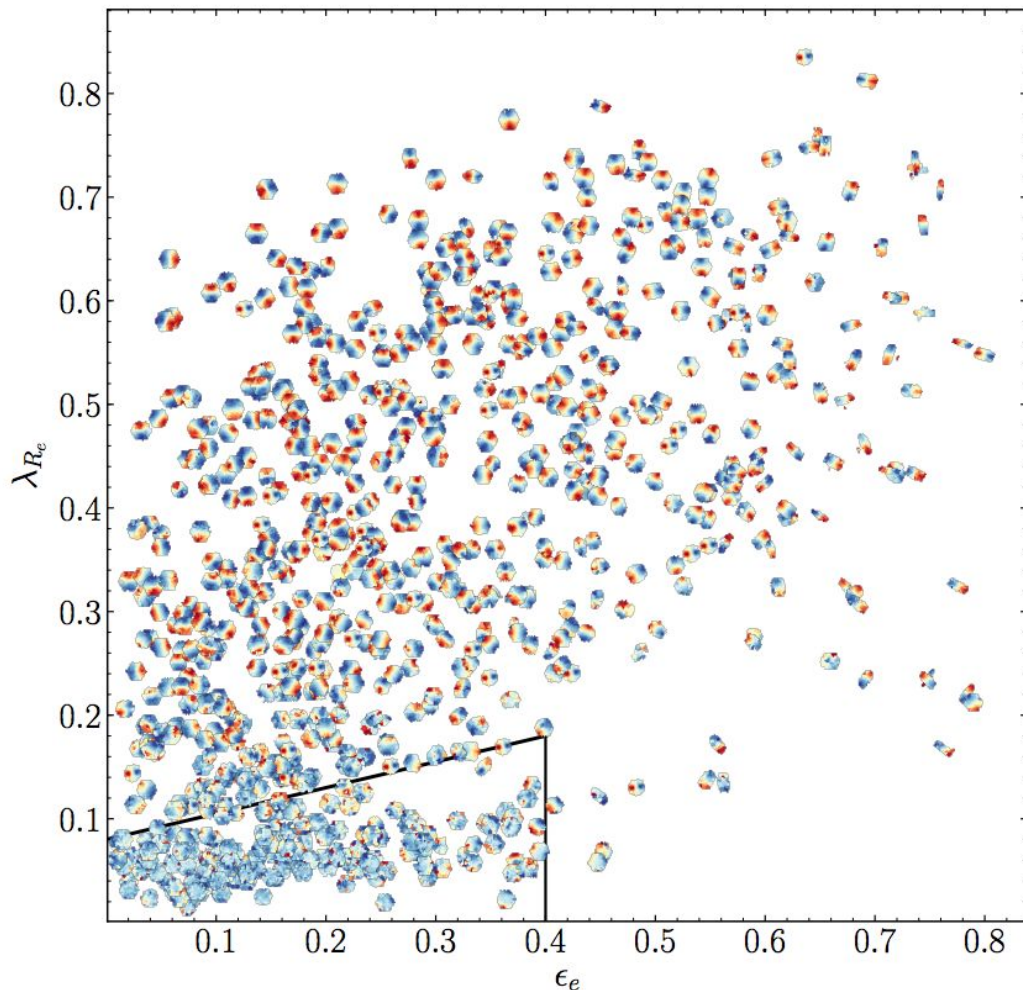


**Figure 1.** Stellar mass against star formation rate for the Q-MANGA-GALEX sample with regular (black circles) and non-regular (red squares) rotators identified using Equation 2. Shown also are the contours for the entire MPA-JHU sample (grey contours; i.e. SDSS DR7). The solid line shows the SFS as defined by Peng et al. (2010) at the average redshift of the Q-MANGA-GALEX sample, with  $\pm 1\sigma$  shown by the dashed lines. Note that the galaxies in the Q-MANGA-GALEX sample are chosen to be more than  $1\sigma$  below the SFS as defined at their observed redshift and stellar mass (see Section 2.3).

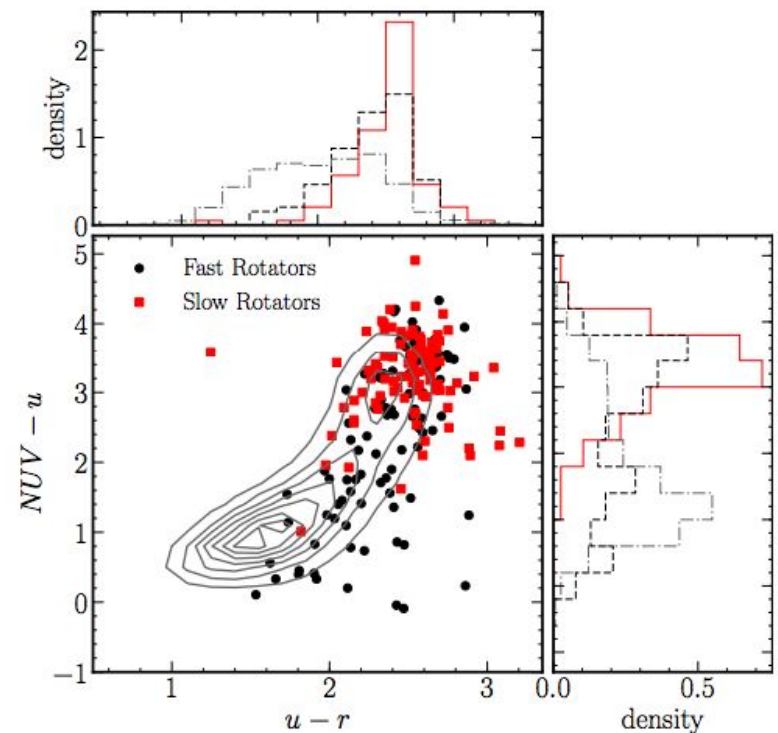
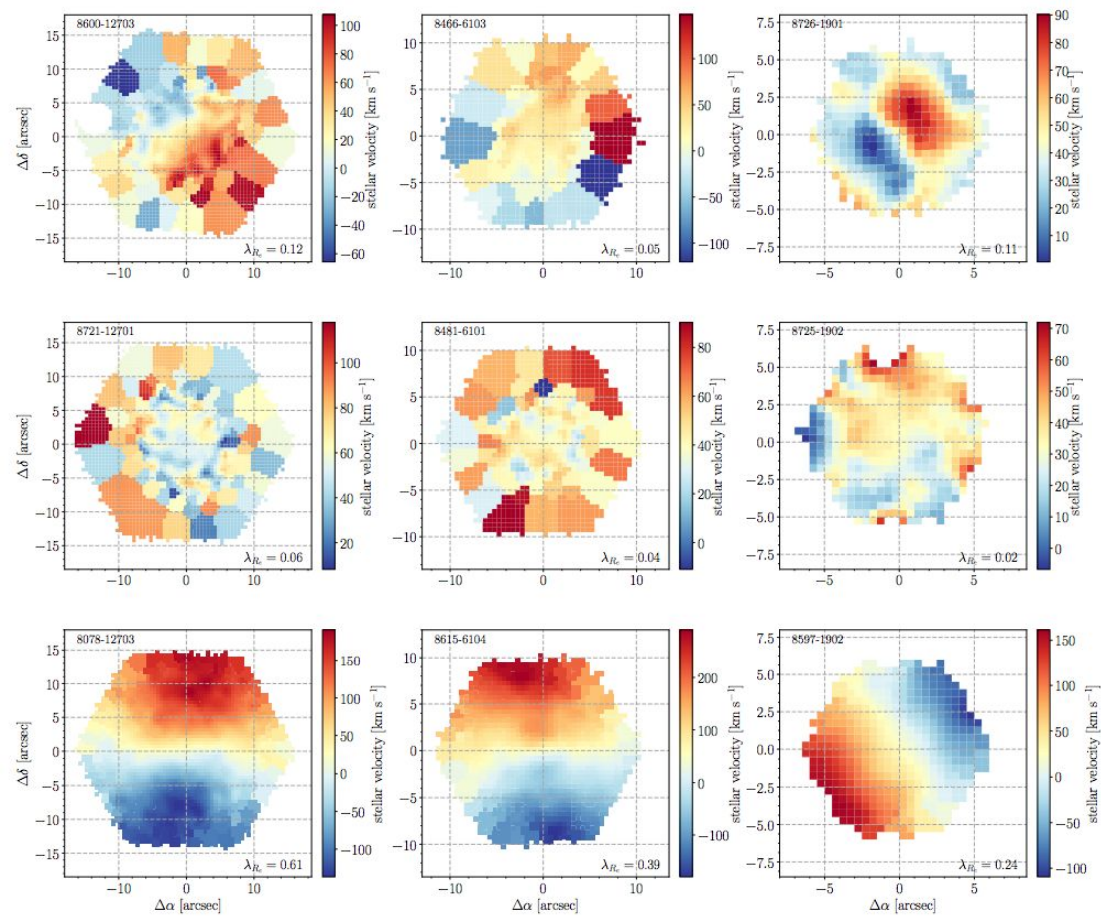
Using this definition reveals 168 (20%) non-regular rotators and 658 (80%) regular rotators in the q-manga-galex sample.

826 quenching or quenched galaxies

$$\lambda_{R_e} = \frac{\sum_{i=1}^N F_i R_i |V_i|}{\sum_{i=1}^N F_i R_i (V_i^2 + \sigma_i^2)^{1/2}}$$



In order to obtain a sample of slow rotators, one author (RJS) inspected the velocity maps of the 168 non-regular rotators identified in the Q-MANGA-GALEX sample to remove those galaxies which showed rotation in their kinematic map (i.e. counter rotation or decoupled cores). 71 galaxies exhibiting rotation were identified, example velocity maps for which are shown in the top row of Figure 3. This resulted in a sample of 97 slow rotators, example velocity maps for which are shown in the middle row of Figure 3.



## 2.6 Star Formation History Inference

STARPY<sup>3</sup> is a PYTHON code which allows the inference of the exponentially declining star formation history (SFH) of a single galaxy using Bayesian Markov Chain Monte Carlo techniques (Foreman-Mackey et al. 2013)<sup>4</sup>. The code uses the solar metallicity stellar population models of (Bruzual & Charlot 2003, hereafter BC03), assumes a Chabrier IMF (Chabrier 2003) and requires the input of the observed  $u-r$  and  $NUV-u$  colours and redshift. No attempt is made to model for intrinsic dust.

The SFH is described by an exponentially declining SFR described by two parameters; the time at the onset of quenching,  $t_q$  [Gyr], and the exponential rate at which quenching occurs,  $\tau$  [Gyr]. Under the simplifying assumption that all galaxies formed at  $t = 0$  Gyr with an initial burst of star formation, the SFH can be described as:

$$SFR = \begin{cases} i_{sfr}(t_q) & \text{if } t < t_q \\ i_{sfr}(t_q) \times \exp\left(\frac{-(t-t_q)}{\tau}\right) & \text{if } t > t_q \end{cases} \quad (3)$$

where  $i_{sfr}$  is an initial constant star formation rate dependent on  $t_q$  (Schawinski et al. 2014; Smethurst et al. 2015). The simplifying assumption that all galaxies formed at  $t = 0$  Gyr means that the age of each galaxy,  $t_{age}$ , corresponds to the age of the Universe at its observed redshift,  $t_{obs}$ . A smaller  $\tau$  value corresponds to a rapid quench, whereas a larger  $\tau$  value corresponds to a slower quench. A galaxy undergoing a slow quench is not necessarily quiescent

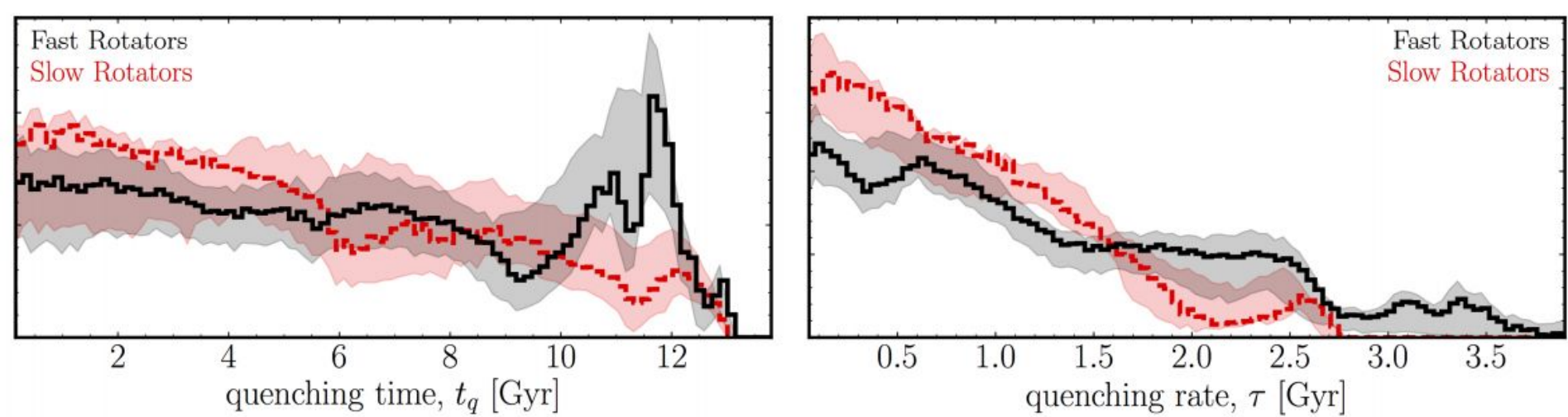


**Figure 5.** Population densities for the time,  $t_q$  (left) and exponential rate,  $\tau$  (right) that quenching occurs in the MM-Q-MANGA-GALEX sample for the fast (black, solid) and slow (red, dashed) rotators. A high value of  $t_q$  corresponds to a recent quench, and a high value of  $\tau$  corresponds to a slow quench. Shaded regions show the uncertainties on the distributions from bootstrapping.

- An Anderson-Darling test revealed that the distribution of the inferred quenching rates of fast and slow rotators are **statistically distinguishable** ( $p = 0.001$ ,  $3.2\sigma$ ). We find that **rapid quenching rates** ( $\tau \sim < 1$  Gyr) **are dominant for slow rotators**, supporting the theory that slow rotators form in **dynamically fast processes**, such as major mergers (Bois et al. 2010; Duc et al. 2011; Naab et al. 2014).
- we find that **fast rotators** quench at a wide range of rates, consistent with **dynamically slow processes** such as secular evolution, minor mergers, gas accretion and environmentally driven mechanisms.
- However we also find evidence that **some of the fast rotators** are quenching **at the same rapid rates** dominant across the slow rotator sample.
- This finding of rapid quenching rates occurring for both slow rotators and a subset of the fast rotators suggests that although their kinematics are different in nature, both classes of galaxy may be able to quench, and therefore form, via major mergers. This result combined with the findings of recent simulations showing disc survival in gas-rich major mergers (Bois et al. 2011; Pontzen et al. 2016; Sparre & Springel 2016), suggests that the total gas mass fraction within a pair of merging galaxies, is what will ultimately decide the kinematic fate of a galaxy.

A  $^{13}\text{CO}$  DETECTION IN A BRIGHTEST CLUSTER GALAXY

A. N. VANTYGHM<sup>1</sup>, B. R. MCNAMARA<sup>1,2</sup>, A. C. EDGE<sup>3</sup>, F. COMBES<sup>4,5</sup>, H. R. RUSSELL<sup>6</sup>, A. C. FABIAN<sup>6</sup>, M. T. HOGAN<sup>1,2</sup>, M. MCDONALD<sup>7</sup>, P. E. J. NULSEN<sup>8,9</sup>, AND P. SALOMÉ<sup>4</sup>

<sup>1</sup> Department of Physics and Astronomy, University of Waterloo, Waterloo, ON N2L 3G1, Canada; [a2vantyg@uwaterloo.ca](mailto:a2vantyg@uwaterloo.ca)

<sup>2</sup> Perimeter Institute for Theoretical Physics, Waterloo, Canada

<sup>3</sup> Department of Physics, Durham University, Durham DH1 3LE

<sup>4</sup> LERMA, Observatoire de Paris, CNRS, UPMC, PSL Univ., 61 avenue de l'Observatoire, 75014 Paris, France

<sup>5</sup> Collège de France, 11 place Marcelin Berthelot, 75005 Paris

<sup>6</sup> Institute of Astronomy, Madingley Road, Cambridge CB3 0HA

<sup>7</sup> Kavli Institute for Astrophysics and Space Research, Massachusetts Institute of Technology, 77 Massachusetts Avenue, Cambridge, MA 02139, USA

<sup>8</sup> Harvard-Smithsonian Center for Astrophysics, 60 Garden Street, Cambridge, MA 02138, USA

<sup>9</sup> ICRAR, University of Western Australia, 35 Stirling Hwy, Crawley, WA 6009, Australia

*Draft version September 29, 2017*

## ABSTRACT

We present ALMA Cycle 4 observations of CO(1-0), CO(3-2), and  $^{13}\text{CO}(3-2)$  line emission in the brightest cluster galaxy of RXJ0821+0752. This is one of the first detections of  $^{13}\text{CO}$  line emission in a galaxy cluster. Half of the CO(3-2) line emission originates from two clumps of molecular gas that are spatially offset from the galactic center. These clumps are surrounded by diffuse emission that extends 8 kpc in length. The detected  $^{13}\text{CO}$  emission is confined entirely to the two bright clumps, with any emission outside of this region lying below our detection threshold. Two distinct velocity components with similar integrated fluxes are detected in the  $^{12}\text{CO}$  spectra. The narrower component (60 km s<sup>-1</sup> FWHM) is consistent in both velocity centroid and linewidth with  $^{13}\text{CO}(3-2)$  emission, while the broader (130–160 km s<sup>-1</sup>), slightly blueshifted wing has no associated  $^{13}\text{CO}(3-2)$  emission. A simple local thermodynamic model indicates that the  $^{13}\text{CO}$  emission traces  $2.1 \times 10^9 M_{\odot}$  of molecular gas. Isolating the  $^{12}\text{CO}$  velocity component that accompanies the  $^{13}\text{CO}$  emission yields a CO-to-H<sub>2</sub> conversion factor of  $\alpha_{\text{CO}} = 2.3 M_{\odot} (\text{K km s}^{-1})^{-1}$ , which is a factor of two lower than the Galactic value. Adopting the Galactic CO-to-H<sub>2</sub> conversion factor in brightest cluster galaxies may therefore overestimate their molecular gas masses by a factor of two. This is within the object-to-object scatter from extragalactic sources, so calibrations in a larger sample of clusters are necessary in order to confirm a sub-Galactic conversion factor.

*Keywords:* galaxies: active — galaxies: clusters: individual (RXJ0821+0752) — galaxies: ISM — radio lines: ISM